Measurement 43 (2010) 1656–1660

Contents lists available at ScienceDirect

Measurement

journal homepage: www.elsevier.com/locate/measurement

Optimization of parameters acting on a projectile velocity within a four stage induction coil-gun

Ismail Coşkun [a], Osman Kalender [b,*], Yavuz Ege [c], Sedat Nazlibilek [d]

[a] Gazi University, Department of Electric-Electronics Engineering, 06500 Besevler/Ankara, Turkey
[b] Communications and Electronics Systems Branch, 06100 Bakanliklar, Ankara, Turkey
[c] Balikesir University, Necatibey Faculty of Education, Department of Physics, 10100 Balikesir, Turkey
[d] Atilim University, Department of Mechatronics Engineering, 06100 Ankara, Turkey

ARTICLE INFO

Article history:
Received 8 June 2009
Received in revised form 31 August 2010
Accepted 3 September 2010
Available online 15 September 2010

Keywords:
Coil gun
Fire timing
Projectile material
Projectile speed

ABSTRACT

In this work, a four stage induction coil-gun has been designed and the parameters acting on the bullet velocity has been investigated. The mutual inductance variation depending on the bullet coil position, determination of firing point exposed to the maximum force with respect to the length, and appropriate material selection for the bullet coil have been analyzed. Optimum solutions for these parameters have been presented.

1. Introduction

Coil-guns are electromagnetic guns that use the by Lorentz *(JxB)* force to accelerate a projectile with a conducting armature. In recent years, the developments on the power electronics have provided important progress in the area of applications of electromagnetic coil-guns. The multi-stage induction coil-guns among the electromagnetic weapons with different types [1,2] and different working principles [3–9] might be considered as the guns having greater expectancy in the near future [10–12]. In our study, a micro-controller controlled, four stage induction coil-gun with new characteristics has been designed.

In this paper, after giving a short presentation of the system developed, the effects of the geometry of the coils within the firing assembly of the system, the material used to manufacture the coil, and the firing point on the velocity reached with the system are investigated and the results are discussed in detail.

2. The design approach for the system

The induction coil-gun developed here is composed of an electromagnetic firing assembly made up of a four-stage driver coil set, an electronic switching circuit using thyristors, and a measurement and control system utilizing a micro-controller and a computer. The system block diagram can be seen in Fig. 1. The electrical equivalent circuit for one stage is shown in Fig. 2 where L_d is the driver coil inductance, I_d is the current passing through it and R_d is the internal resistance of it, L_p is the inductance of the rotor coil, I_p is the current and R_d is the resistance of it. The voltage charged in the capacitor C is discharged through the driver coil by means of the switch S. The magnetic field created within the driver coil induces a voltage on the projectile coil. Since the current passing through the projectile coil is in the opposite direction to the current of the driver, a pushing force is created. If the mutual inductance between the two coils is M and the pushing force between the two coils is F_m, then the magnitude of this force can be found by the Eq. (1) in accordance with the Lenz Law as follows:

* Corresponding author. Fax: +90 3124175190.
E-mail address: drosmankalender@gmail.com (O. Kalender).

0263-2241/$ - see front matter © 2010 Elsevier Ltd. All rights reserved.
doi:10.1016/j.measurement.2010.09.020

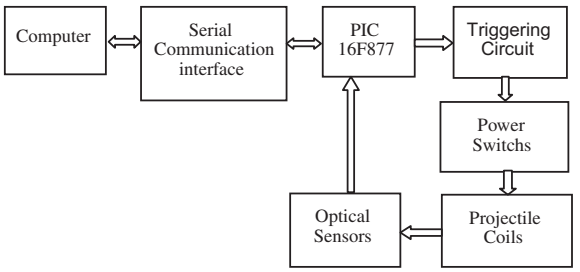

Fig. 1. The block diagram of the induction coil-gun.

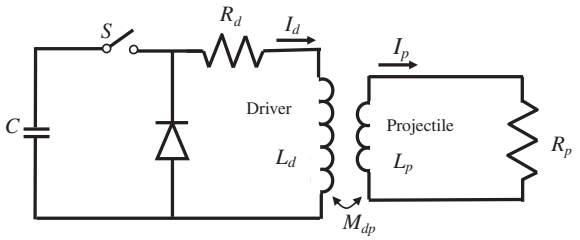

Fig. 2. The circuit diagram of the induction coil-gun.

$$F_p = I_d I_p \frac{dM}{dx} \tag{1}$$

As you notice that the effects of geometries of the driver and projectile coils, operating voltage, the slope of the mutual inductance between the two coils, electrical and magnetic properties of the material used, and the power source supplying the circuit on the velocities achieved by the induction coil-gun developed could be large enough.

A conventional driver and projectile types used in the applications of induction coil-gun are depicted in Fig. 3. The partial 3D FEM model belonging to the coils and their electrical equivalent network are shown in Fig. 4.

In order to simulate the effect of driver coil geometry on the mutual inductance and magnetic flux, some experiments are carried out by changing the ratio of r_{d2}/r_{d1}. A d.c. current of 1 A is applied to the stator coil and it is seen that although the value of the current was not changed, the flux of the stator has been increased in parallel with the increase in the ratio r_{d2}/r_{d1}. However, the value of the mutual inductance has decreased. The boundary conditions have been defined as 6.5 times that of the coil length as shown in Fig. 5, where the energy is assumed to be zero.

The results of the simulation can be seen in Fig. 6.

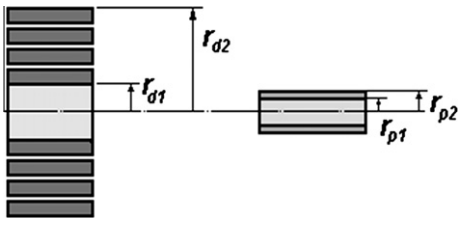

Fig. 3. Conventional type driver and projectile coils.

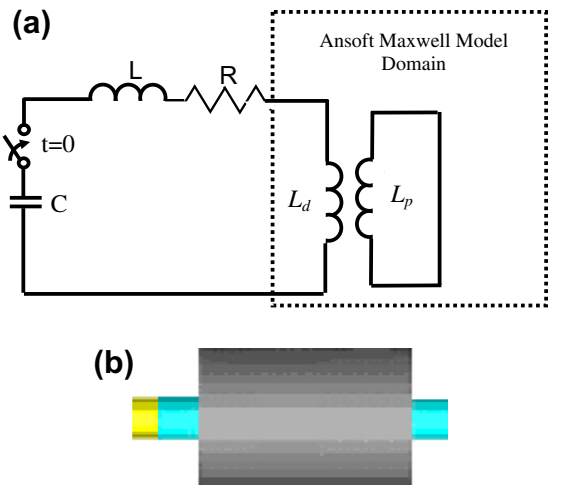

Fig. 4. Conventional driver and projectile coil model. (a) Electrical equivalent network. (b) The partial 3D FEM model.

Under the same simulation conditions, the ratio r_{p2}/r_{p1} of the projectile coil has been changed in order to see the effects of the projectile coil geometry on the mutual inductance and magnetic flux linkage. The results are shown in Fig. 7.

When we look at the simulation results in Figs. 6 and 7, we conclude that the stator and projectile coils need to be close to each other and the magnetic flux path passing through the stator coil must not be away from the projectile coil.

In our practical work, the driver coil developed is made up of wounds in the shape of a toroid as seen in Fig. 8. In such a coil, the magnetic flux (Φ) can be found by Eq. (2).

For Φ along the coil

$$\Phi = \int \vec{B} \cdot d\vec{S}$$

$$\Phi = \frac{\mu_0 i_0 N}{2\pi} \int_{r_{d1}}^{r_{d2}} \int_0^h \int_0^{2\pi} \frac{1}{2} d_r d_z d_\Phi$$

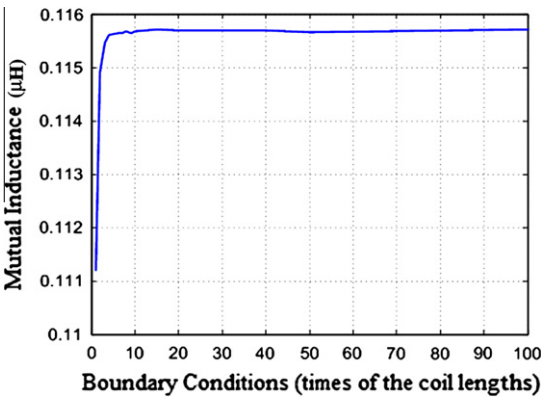

Fig. 5. The changes of boundary conditions, depending of mutual inductance.

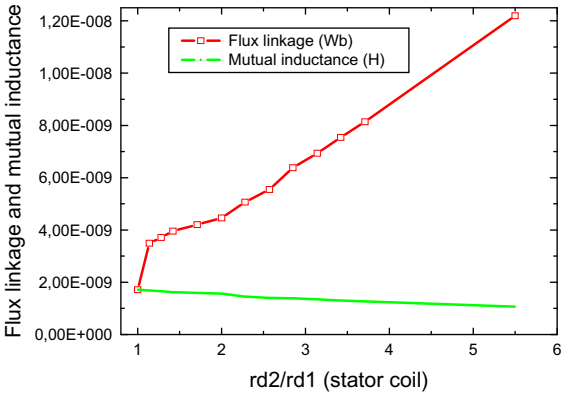

Fig. 6. Flux linkage and mutual inductance changes depending on the ratio r_{d2}/r_{d1} of the stator coil.

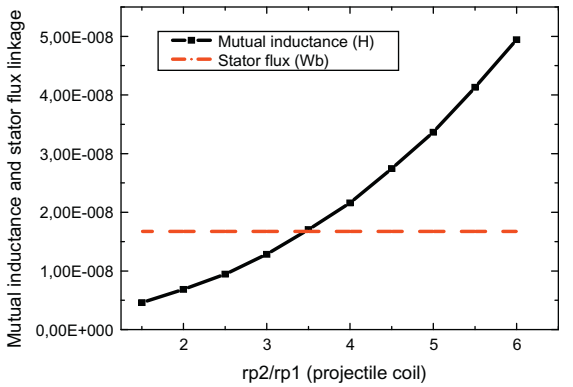

Fig. 7. Flux linkage and mutual inductance change depending on the ratio r_{p2}/r_{p1} of the projectile coil.

$$\Phi = \frac{\mu_0 i_0 N h}{2\pi} \quad \ln\frac{r_{d2}}{r_{d1}} \tag{2}$$

With a coil sequence of length l, the mutual inductance between the stator and projectile coils can be calculated by the following equation:

$$M_{dp} = \frac{\Phi_p}{I_d} = \frac{\mu_0 N_d N_p \pi r^2}{l} \tag{3}$$

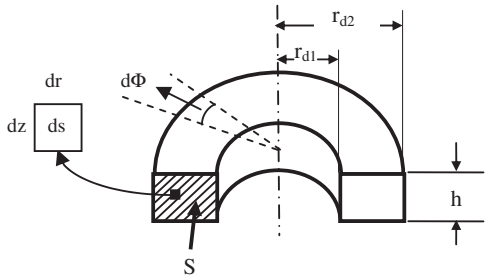

Fig. 8. Toroid shaped coil.

We notice from the Eqs. (2) and (3) that the flux Φ and the mutual inductance depend on the coil geometry. Furthermore, this situation is in line with the simulation results.

The driver coil wounds used in this study are identical to the wounds used in conventional driver coils, but since they are in the shape of a toroid, they have a capability to intensify the flux. The driver and projectile coil geometries designed in this work are shown in Fig. 9. The partial 3D FEM model of this coil is given in Fig. 10.

The appearance of the induction coil-gun developed in this work can be seen in the photograph (Fig. 11).

The length of the driver coil is 38 mm and the length of the projectile coil is 10 mm for the induction coil-gun system developed here. During the design phase of the system, the following steps have to be followed.

a. The mutual inductance change depending on the projectile position has to be determined.
b. Based on the length of the projectile coil, the firing point where the projectile is subject to the maximum force has to be determined.
c. Suitable material for the projectile coil has to be selected.

The findings are given in the following section.

3. Findings

First of all, the simulation results for the mutual inductance between the classical driver coil and the coil having

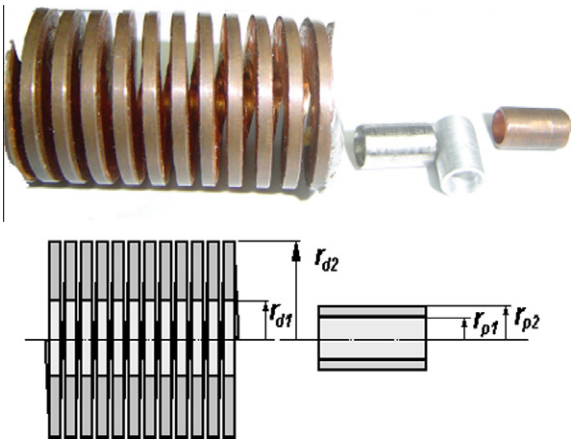

Fig. 9. The driver and projectile coil geometries designed in this work.

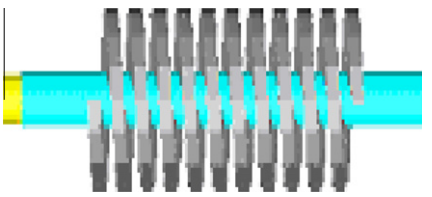

Fig. 10. Simulation model.

Fig. 11. The appearance of the induction coil-gun developed in this work.

flux intensifying capability used in our system, and for the change in mutual inductance are determined at the experiments. These results are presented in Fig. 12.

As seen in Fig 12, the driver coil having the type of a flux intensifying coil provides larger change in mutual inductance with the same power conditions and depending on this larger push force to the projectile can be obtained.

The middle point of the driver coil at the horizontal axis is the point shown as the zero point. When the projectile reaches this point, the mutual inductance between the projectile coil and the driver coil increases and reaches its maximum value. As the projectile moves in the direction of the output of the driver coil, the mutual inductance decreases. The change in the mutual inductance during the motion of the projectile within the driver coil increases in both positive and negative directions as seen from the

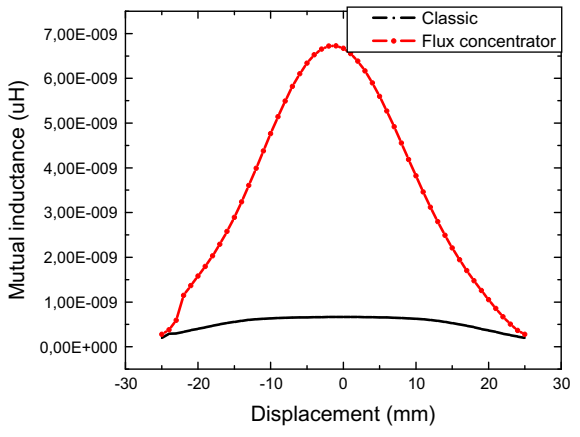

Fig. 12. Mutual inductance change depending on projectile position.

curve. This curve is the same as in shape with the curve of the force acting on the projectile. In other words, the projectile is pushed to the out in both directions on every point where the position is not zero.

As seen in Table 1, although the weight of the copper projectile is greater than that of the titanium projectile, the rate of change in velocity is faster than that of the titanium. In this case, if the masses of both projectiles are the same, the increase in the rate at the output will be greater for the copper projectile. At the first glance, someone could think that since the mass of the aluminum projectile is less than the other two projectiles, its velocity increase would be higher. However, this is not the case. This comes from the fact that the rate of increase in velocity is also depend on the electrical conductivity of the material. A decrease in electrical conductivity gives rise to decease in the rate of increase in velocity. For example, the electrical conductivity of aluminum is the 61% of copper. Therefore, as seen from Table 1, the copper projectile mass is 2.335 times greater than the aluminum projectile (0.612/0.266 = 2.335), and this causes that the velocity of the aluminum projectile to increase, however since the conductivity of it is 61% less than the copper, its velocity decreases accordingly. But the overall effect to the velocity increase will be $2.335 * 0.61 = 1.43$. As a result, the rate of increases in velocities for the copper, aluminum and titanium projectiles with the same masses will have the same order in the list shown in Table 1. But the differences between the rate of increase will not be as great as the values shown in table.

As seen also in Table 2, as the length of the aluminum projectile increases, the rate of increase in velocity decreases. The reason for this is that as the length of the projectile increases, the resistance of the projectile increases and depending upon this, I_p and F push force decrease.

4. Conclusion

In this work, a four stage induction coil-gun is designed and practical application is realized. By changing the type of the driver coil in oppose to the types used in classical

Table 1
The speed which has been measured for different materials.

Material	Length of the projectile (mm)	Weight (g)	Initial velocity (m/s)	Output velocity (m/s)	Rate of increase in velocity (%)
Copper	10	0.621	3.794	4.032	106.273
Titanium	10	0.51	5.4	5.593	103.574
Aluminum	10	0.266	1.878	3.915	208.466

Table 2
The speed of the aluminum projectiles that are in different length.

Length of the projectile (mm)	Initial velocity (m/s)	Output velocity (m/s)	Rate of increase in velocity (%)
10	1.878	3.915	208.466
15	2.314	4.711	203.586
20	5.015	7.657	152.681

applications, a greater push force could be obtained with the same power conditions. The driver coil type used in our application is a type having the capability of intensifying magnetic flux.

Our practical system is composed of a capacitor of 2200 μF charged to 750 V d.c. voltage and a coil of 13 turns with the capability of intensifying the magnetic flux. Driver coils are energized by the help of a micro-controller controlled system and particular software developed for this purpose. In order to obtain a maximum efficiency from an induction coil-gun under the operation conditions available in this study, it is seen that a projectile coil made from aluminum with a length of 10 mm is more appropriate solution than the others.

References

[1] D.P. Bauer, A novel railgun launcher design, IEEE Trans. Magn. 3 (1) (1995) 267–272.
[2] M.J. Matyac, F. Christopher, K.A. Jaminson, C. Persad, R.A. Marshall, Railgun performance enhancement from distribution of energy feeds, IEEE Trans. Magn. 31 (1) (1995) 332–337.
[3] S.K. Ingram, Theoretical analysis of a collapsing field accelerator, in: 6th Symposium of Electromagnetic Launch Technology, Austin, Texas, 1992, pp. 28–30.
[4] S. Seely, A.D. Poularikas, Electromagnetics – Classical and Modern Theory and Applications, Marcel Dekker Inc., New York, 1979. pp. 19–21.
[5] R.J. Kaye, Design and performance of Sandia's contactless coilgun for 50 mm projectiles, IEEE Trans. Magn. 29 (1993) 680–685.
[6] J.A. Andrews, Coilgun structures, IEEE Trans. Magn. 29 (1) (1993) 637–642.
[7] S. Williamson, C.D. Horne, D.C. Haugh, Design of pulsed coil-guns, IEEE Trans. Magn. 31 (1) (1995) 516–521.
[8] E.R. Laithwaite, Propulsion Without Wheels, English University Press Ltd., 1966, pp. 74–79.
[9] J. Li et al., Resistance calculation of the reusable linear magnetic flux compressor coil, IEEE Trans. Magn. 41 (1) (2005) 471–473.
[10] I. Coşkun, O. Kalender, Y. Ege, Induksiyon Bobin Silahi için Stator Bobini Geometrisinin Arastirilmasi, Journal of the Institute of Science and Technology of Balikesir University 8 (2) (2006) 40–48.
[11] R.J. Kaye, Operational requirements and issues for coilgun electromagnetic launchers, IEEE Trans. Magn. 41 (1) (2005) 194–199.
[12] K. Kim, Z. Zabar, E. Levi, L. Birenbaum, In-bore projectile dynamics in the linear induction launcher, IEEE Trans. Magn. 31 (1) (1995) 484–488.